ISSN 0036-0244, Russian Journal of Physical Chemistry A, 2023, Vol. 97, No. 3, pp. 514–520. © Pleiades Publishing, Ltd., 2023.
Russian Text © The Author(s), 2023, published in Zhurnal Fizicheskoi Khimii, 2023, Vol. 97, No. 3, pp. 426–433.

PHYSICAL CHEMISTRY OF DISPERSED SYSTEMS AND SURFACE PHENOMENA

Non-Equilibrium Shells around Precipitates During the Decomposition of a Three-Component Alloy

I. K. Razumov[a,*]

[a] *Institute of the Physics of Metals, Russian Academy of Sciences, Ural Branch, Yekaterinburg, 6200990 Russia*

**e-mail: rik@imp.uran.ru, ilya.k.razumoff@gmail.com*

Received May 25, 2022; revised September 1, 2022; accepted September 19, 2022

Abstract—The kinetic theory of diffusion over vacancies is used to obtain expressions for the fluxes of atoms in a three-component alloy. This hole gas approach allows us to express kinetic coefficients in terms of the coefficients of diffusion of labeled atoms from microscopic considerations. The conditions for the formation of non-equilibrium impurity shells are revealed by studying the kinetics of decomposition using these expressions. These shells can considerably inhibit the growth of precipitates and change the properties of the alloy.

Keywords: spinodal decomposition, three-component alloy, impurity shells, microscopic theory of diffusion

DOI: 10.1134/S0036024423030238

INTRODUCTION

The properties of alloys are largely determined by their phase and structural state, which forms at elevated temperatures and remains metastable (kinetically) as a result of subsequent cooling. Alloys based on aluminum [1], titanium [2], and martensitic aging steels [3] containing nanosized precipitates are of particular interest. Interest in αFeCu alloy has grown in recent years [4–6], in which bcc-Cu precipitates coherent with its matrix appear at the initial stages of decomposition. These precipitates strengthen the alloy. When they reach sizes around 10 nm, their lattice is rearranged into fcc and the alloy becomes fragile. It is therefore of interest to find mechanisms for stabilizing the state reached at the intermediate stages of decomposition. It is known that an effective way of controlling the kinetics of decomposition is to use alloying additives [6–12] that affect the thermodynamic stability of the alloy or produce secondary precipitates.

The thermodynamics and kinetics of decomposition in a binary alloy have been thoroughly studied [13]. Depending on the position of the figurative point on the phase diagram, an alloy can decompose according to the nucleation and subsequent growth of precipitates [14], or the growth of long-wavelength fluctuations in the composition (so-called spinodal decomposition [15, 16]). In both cases, the evolution of the alloy at advanced stages is described by the Lifshitz–Slezov equations in [17].

Studies of the kinetics of decomposition in a three-component alloy began relatively recently. A general analysis of the problem was performed in [18], and typical morphologies of the precipitates for an abstract model were identified. It was shown in subsequent works [19–21] that the morphology of precipitates upon decomposition depends strongly on the ratio of the components' mobilities of diffusion. The growth of precipitates can be inhibited as a result of the formation of shells (or precipitates of secondary phases) around primary precipitates under the influence of kinetic or thermodynamic factors. Possible scenarios for the formation of such shells were analyzed in [22].

Despite the progress made in our qualitative understanding of such processes, formulating a relatively simple but consistent kinetic model of decomposition in a three-component alloy is still an urgent task. In [22], the atomic fluxes were determined using a phenomenological approach based on a generalized Fick's law: $J_i = -c_i M_{ij} \nabla(\delta F/\delta c_j)$, where c_i is the concentration of atoms of the ith type, F is the Ginzburg–Landau free energy functional, and M_{ij} are elements of the mobility matrix. Cross elements M_{ij}, $i \neq j$ were taken equal to zero, since they were considered to make a small contribution to the kinetics [13]. Diagonal elements M_{ii} were associated with the coefficients of diffusion of labeled atoms D_i by the Einstein relation $M_{ii} = D_i/kT$, which applies to an ideal solid solution when cross elements M_{ij} can be ignored. The coefficients of diffusion of labeled atoms in turn were taken equal to their own (partial) coefficients of diffusion [23]. As discussed in [24], this approach is of limited applicability even in a binary alloy if there is no flow of matter (the Kirkendall effect [25]), and we must correctly describe the diffusion of atoms in the volume of growing precipitates. A more consistent approach is to

derive expressions for atomic fluxes J_i using the microscopic theory of diffusion.

Expressions for the fluxes of atoms in a binary alloy were obtained in [26–28] using the kinetic theory of diffusion over vacancies (the hole gas approach [29]). The absence of a flux of matter (local equilibrium in the vacancy subsystem) was ensured by requiring $|J_V| \to 0$ for the flow of vacancies, after which the expression for the mutual coefficient of diffusion took the simple form $D = D_A D_B(1 - \Psi c_A c_B)/(D_A c_A + D_B c_B)$, and $\Psi = 0$ for an ideal solid solution. An essentially similar expression was obtained in [30]. We may therefore assume that during the decomposition of a binary alloy, regions form in which the coefficient of mutual diffusion varies from values close to $D = D_A(c_A \to 0) \equiv D_A^0$ (the coefficient of diffusion of impurity A in matrix B) to others close to $D = D_B(c_B \to 0) \equiv D_B^0$ (the coefficient of diffusion of impurity B in matrix A). In [31], the microscopic approach was also generalized to an ordering binary alloy with two equivalent sublattices.

In this work, the approach proposed in [26–28, 31] is generalized to a disordered three-component alloy. Expressions for the flows of atoms are derived, and conditions for the formation of nonequilibrium impurity shells around precipitates that form during decomposition of the alloy are studied.

FORMULATING THE MODEL

Let us identify the concentrations of $c_{i(V)}(\mathbf{r})$ atoms of the sort $i = 1, 2, 3$ and vacancies at lattice site $\mathbf{r}$ with the probabilities of their detection at this site, from which $c_V + \sum_{i=1}^{3} c_i = 1$ follows in particular. We assume that diffusion proceeds according to a vacancy mechanism, an atom can jump only to the position of one of its nearest neighbors, and pair correlations in the distribution of atoms can be ignored. The equations for the evolution of concentrations then have the form

$$\frac{dc_i}{dt}(\mathbf{r}) = \sum_{l=1}^{Z} \nu_i(\mathbf{r} + \mathbf{a}_l \to \mathbf{r}) c_V(\mathbf{r}) c_i(\mathbf{r} + \mathbf{a}_l) - \nu_i(\mathbf{r} \to \mathbf{r} + \mathbf{a}_l) c_V(\mathbf{r} + \mathbf{a}_l) c_i(\mathbf{r}). \quad (1)$$

Equation (1) essentially expresses the balance of matter: the change (per unit of time) in the probability of finding an atom of type i at site $\mathbf{r}$ is the sum of the probabilities of atoms of this type jumping from all nodes of the immediate environment to this site, minus those of the reverse jumps. The transitional frequencies are determined according the formulas

$$\nu_i(\mathbf{r} + \mathbf{a}_l \to \mathbf{r}) = \nu_{i0} \exp[(E_i(\mathbf{r} + \mathbf{a}_l) - E_i^s)/kT],$$
$$\nu_i(\mathbf{r} \to \mathbf{r} + \mathbf{a}_l) = \nu_{i0} \exp[(E_i(\mathbf{r}) - E_i^s)/kT], \quad (2)$$

where $E_i(\mathbf{r})$ is the energy of bonding with the environment of an atom of type i located at a site with radius vector $\mathbf{r}$, and E_i^s is the energy of an atom at the saddle point (for simplicity, we assume $E_\sigma^S = \text{const}$).

Assuming that concentrations $c_{i(V)}(\mathbf{r})$ change slowly at distances on the order of a, we expand (1) into a series in $\mathbf{a}_l$ and write the equations of evolution, confining ourselves to the first nonvanishing terms:

$$\frac{dc_i}{dt} = -\nabla \mathbf{J}_i, \quad (3)$$

$$\mathbf{J}_i = \omega_i c_i c_V \nabla[\ln(c_V/c_i) - \nabla E_i/kT], \quad \omega_i = \frac{Za^2}{2}\nu_i. \quad (4)$$

Here we use condition $\sum_s \mathbf{a}_s = 0$ that arises due to the symmetry of the lattice nodes with respect to the one selected, so the equations of diffusion are defined by expansion terms that were quadratic in a.

Let us determine the energy of an atom in the ground state by summing energies $\varphi^{\alpha\beta}(r)$ of pairwise interaction over nodes k of the entire lattice:

$$E_i(\mathbf{r}) = \sum_{j=1}^{3} \sum_k \varphi^{ij}(\xi_k) c_j(\mathbf{r} + \xi_k). \quad (5)$$

Expanding (5) into a series according to ξ_k, we obtain

$$E_i(\mathbf{r}) = \sum_{j=1}^{3} \Phi_{ij}(c_j(\mathbf{r}) + R^2 \Delta c_j(\mathbf{r})),$$
$$\Phi_{ij} = \sum_k \varphi^{ij}(\xi_k). \quad (6)$$

Small parameter R in expression (6) characterizes the effective radius of interatomic interaction. For simplicity, we consider it to be independent of the type of atoms. Terms of order R^2 are needed to describe the evolution of concentrations in the region of interphase boundaries. Strictly speaking, long-range nature $R \gg a$ of interactions is assumed. Otherwise, we would have to expand (4) to the corresponding order in parameter a.

Since the flows of atoms and vacancies are connected by the condition

$$\mathbf{J}_V + \sum_{i=1}^{3} \mathbf{J}_i = 0, \quad (7)$$

we add the fluxes of atoms and express ∇c_V in (4) through $\mathbf{J}_V$. Assuming that the alloy is enclosed in a vessel with fixed walls and there are no sources or sinks of nonequilibrium vacancies, we make the limit transition $\mathbf{J}_V \to 0$. This means transformations occur under conditions of local equilibrium in the vacancy subsystem, so $\mathbf{J}_V \ll \mathbf{J}_i$. We also assume that the concentration of vacancies is low, $c_V \ll c_i$. We then obtain expressions for the flows of atoms:

$$\mathbf{J}_3 \approx -(\mathbf{J}_1 + \mathbf{J}_2), \quad (8)$$

$$\mathbf{J}_1\left(\sum_{i=1}^{3}\omega_i c_i\right) = \sum_{j=2,3}[\omega_1 c_V(\omega_j c_1 + \omega_2 c_2 + \omega_3 c_3)\nabla c_j - \omega_1\omega_j c_V c_1 c_j \Psi_{1j}(\nabla c_j + R^2\nabla\Delta c_j)] - \omega_1 c_V c_1(\Psi_{12} + \Psi_{13} - \Psi_{23})[\omega_2 c_2(\nabla c_3 + R^2\nabla\Delta c_3) + \omega_3 c_3(\nabla c_2 + R^2\nabla\Delta c_2)]/2, \quad (9)$$

$$\mathbf{J}_2\left(\sum_{i=1}^{3}\omega_i c_i\right) = \sum_{j=1,3}[\omega_2 c_V(\omega_j c_2 + \omega_1 c_1 + \omega_3 c_3)\nabla c_j - \omega_2\omega_j c_V c_2 c_j \Psi_{2j}(\nabla c_j + R^2\nabla\Delta c_j)] - \omega_2 c_V c_2(\Psi_{21} + \Psi_{23} - \Psi_{13})[\omega_1 c_1(\nabla c_3 + R^2\nabla\Delta c_3) + \omega_3 c_3(\nabla c_1 + R^2\nabla\Delta c_1)]/2, \quad (10)$$

where $\Psi_{ij} = (2\Phi_{ij} - \Phi_{ii} - \Phi_{jj})/kT$. When $c_3 = 0$, $c_1 + c_2 = 1$, and $\mathbf{J}_1 = -\mathbf{J}_2$ in a binary alloy, formula (9) is reduced to the expression obtained in [26–28], which is qualitatively similar to the expression for the atomic flux in the phenomenological Cahn–Hilliard model of spinodal decomposition [15]:

$$\mathbf{J}_1 = -\frac{\omega_1\omega_2 c_V}{\omega_1 c_1 + \omega_2 c_2}[(1 - \Psi_{12}c_1 c_2)\nabla c_1 - \Psi_{12}c_1 c_2 R^2\nabla\Delta c_1]. \quad (11)$$

Based on the definition of the coefficient of diffusion of labeled atoms (the coefficient of impurity diffusion) through Fick's law $\mathbf{J}_i = -D_i\nabla c_i$ in the limit of low concentrations $c_i \to 0$, we obtain from (11)

$$D_i^0 = \omega_i(c_i \to 0)c_V(c_i \to 0). \quad (12)$$

The coefficients of diffusion of labeled atoms generally depend on the concentrations of components in the alloy. In accordance with formulas (2) and (5), this dependence obeys the Arrhenius law

$$D_i = D_{0i}^0 \exp\left[\sum_{j=1}^{3}\Phi_{ij}c_j/(kT)\right]. \quad (13)$$

Since the coefficient of impurity diffusion in pure substances is $D_i(c_j \to 1) \equiv D_{ij}^0$ and the self-coefficient of diffusions $D_i(c_i \to 1) \equiv D_{ii}^0$ are known from experiments, we rewrite (13) in the equivalent form

$$D_i = (D_{i1}^0)^{c_1}(D_{i2}^0)^{c_2}(D_{i3}^0)^{c_3}. \quad (14)$$

We finally rewrite the expressions for the flows of atoms (8) and (9) using D_i instead of ω_i:

$$\mathbf{J}_1\left(\sum_{i=1}^{3}D_i c_i\right) = \sum_{j=2,3}[D_1(D_j c_1 + D_2 c_2 + D_3 c_3)\nabla c_j - D_1 D_j c_1 c_j \Psi_{1j}(\nabla c_j + R^2\nabla\Delta c_j)] - D_1 c_1(\Psi_{12} + \Psi_{13} - \Psi_{23})[D_2 c_2(\nabla c_3 + R^2\nabla\Delta c_3) + D_3 c_3(\nabla c_2 + R^2\nabla\Delta c_2)]/2, \quad (15)$$

$$\mathbf{J}_2\left(\sum_{i=1}^{3}D_i c_i\right) = \sum_{j=1,3}[D_2(D_j c_2 + D_1 c_1 + D_3 c_3)\nabla c_j - D_2 D_j c_2 c_j \Psi_{2j}(\nabla c_j + R^2\nabla\Delta c_j)] - D_2 c_2(\Psi_{21} + \Psi_{23} - \Psi_{13})[D_1 c_1(\nabla c_3 + R^2\nabla\Delta c_3) + D_3 c_3(\nabla c_1 + R^2\nabla\Delta c_1)]/2. \quad (16)$$

The solution to the system of Eqs. (3), (15), and (16), which describes the evolution of the concentrations of an alloy's components under known initial and boundary conditions, can be obtained numerically. The coefficient of diffusion of labeled atoms can be calculated for a particular alloy from experimental data using formula (14), and energies of interaction Ψ_{ij} can be calculated using data from first-principle calculations.

We can use the integral degree of decomposition with respect to component i to analyze the kinetics of transformation:

$$S_{\text{dec}}^{(i)}(t) = \frac{1}{2c_{i0}(1 - c_{i0})L^d}\int|c_i(\mathbf{r}, t) - c_{i0}|d\mathbf{r}, \quad (17)$$

where d is the dimension of the problem, L is the size of the sample, c_{i0} is the average concentration of the component i over the sample, and $0 \le S_{\text{dec}}^{(i)} \le 1$.

KINETICS OF ALLOY DECOMPOSITION AND THE FORMATION OF SHELLS AROUND PRECIPITATES

We shall limit ourselves to analyzing solutions to systems (3), (15), (16) on a 1D region using an explicit two-layer finite-difference scheme, with dimensionless time $\tau = tD_{11}^0/L^2$ and coordinate x/L. The initial state was chosen to be homogeneous with average concentrations c_{i0} and a small perturbation in the center of the computational domain using mirror-symmetric boundary conditions (i.e., the absence of component flows through the boundaries of the computational domain).

The results in [22] show that the kinetics of decomposition in a three-component alloy allows a wide variety of scenarios, depending on the ratios of parameters of interatomic interaction Ψ_{ij} and coefficient of diffusion D_{ij}^0. Let us consider typical scenarios in which $\Psi_{12} > 0$ and $c_{10} < c_{20}$, so precipitation based on component **1** forms in the matrix based on component **2**. The values of the coefficient of diffusion in the calculations below made dimensionless by dividing by D_{11}^0.

When $\Psi_{13} > 0$, $\Psi_{23} = 0$, component **3** is displaced from the volume of precipitate into the matrix as the precipitate grows. If the coefficient of diffusion of components D_{12}^0 and D_{32}^0 in a matrix are comparable, component **3** has time to be almost uniformly distributed in the matrix as precipitation grows (Fig. 1a). If

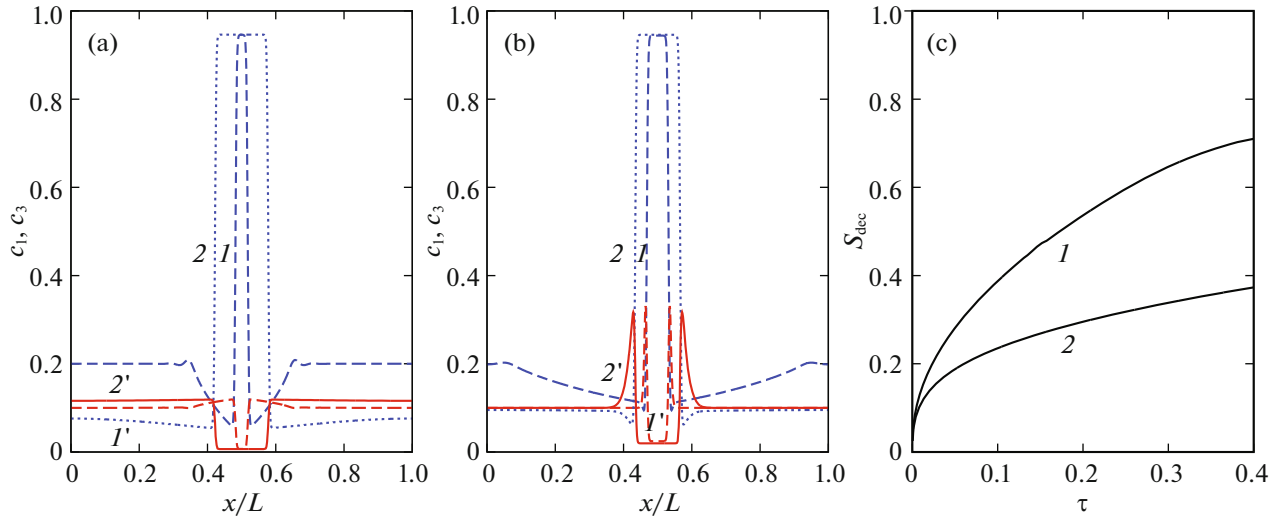

Fig. 1. Kinetics of precipitate growth in an alloy with parameters $\Psi_{12} = \Psi_{13} = 6.5$, $\Psi_{23} = 0$, $c_{10} = 0.2$, $c_{30} = 0.1$, and $L = 500R$. (a) Distributions of concentrations (*1*, *2*) $c_1(x)$ and (*1'*, *2'*) $c_3(x)$ at times τ = (*1*, *1'*) 0.01 and (*2*, *2'*) 0.4 when $D_{ij}^0 = 1$; (b) distributions of concentrations (*1*, *2*) $c_1(x)$ and (*1'*, *2'*) $c_3(x)$ at times τ = (*1*, *1'*) 0.17 and (*2*, *2'*) 2 when $D_{32}^0 = D_{33}^0 = 10^{-4}$; for all others, $D_{ij}^0 = 1$; (c) evolution of decomposition with respect to component **1** for (a) and (b), respectively.

$D_{12}^0 \gg D_{32}^0$, component **3** remains near its surface in the form of a nonequilibrium shell that takes a long time to dissolve up to the point where the precipitation finishes growing (Fig. 1b). A comparison of the evolution of decomposition in these two cases (Fig. 1c) shows that the slow diffusion of component **3** that forms the shell slows the growth of the precipitate, since the growth of the precipitate implies the movement of the shell.

In contrast, component **3** is displaced from the matrix into the volume of the precipitate as it grows when $\Psi_{23} > 0$ and $\Psi_{13} = 0$. If coefficients of diffusion D_{12}^0 and D_{31}^0 are comparable, component **3** is almost uniformly distributed in the precipitate volume at all stages (Fig. 2a). If $D_{12}^0 \gg D_{31}^0$, the central part of the precipitate is largely depleted in component **3** by the time it finishes growing, while a layer enriched in this component forms in the near-boundary area (Fig. 2b). A comparison of the evolution of decomposition in these cases shows that an additional condition is needed to slow the growth of the precipitate: $D_{13}^0 \ll D_{12}^0$, meaning that the penetration of type *1* atoms of through the shell is hindered (Fig. 2c).

Note that in the example presented here, the growth of the precipitate is slowed under the conditions of maintaining the supersaturated state in the matrix. With an ensemble of precipitates, we can also consider the slowing of the kinetics of decomposition at a later stage, when large precipitates grow at the expense of small ones under conditions of a local equilibrium in the matrix at constant degree of decomposition S_{dec} (the so-called evaporation–condensation stage) [17].

The data presented in Figs. 1 and 2 show that nonequilibrium shells form around precipitates when, as a result of the action of a thermodynamic stimulus to decomposition, impurity atoms are displaced into the phase in which their diffusion mobility is reduced. The drop in the coefficient of diffusion of the atoms that form the precipitate in the region of such a shell then helps inhibit the growth of precipitates.

RESULTS AND DISCUSSION

Expressions for atomic flows (15) and (16) have a more complex form than ones written in the phenomenological approach [22], since they offer a derivation of the kinetic coefficients in front of concentration gradients ∇c_i that is derived from microscopic theory. The phenomenological approach can be used in most cases involving only the formation of precipitates of one or several phases (i.e., the effects caused by the thermodynamic properties of the alloy). However, when analyzing effects associated with the ratio of kinetic coefficients, including the formation of nonequilibrium shells, it is better to rely on expressions derived for flows (15) and (16) using the microscopic theory.

A nonequilibrium shell hindering decomposition that was qualitatively similar to the one described above (Fig. 2b) was clearly observed in a three-component Al–Sc–Zr alloy with 0.09 at % Sc and 0.03 at % Zr using a 3D atom probe, high resolution electron microscopy (HREM), and small angle X-ray scattering (SAXS) [19]. It was shown that at $T = 400$–550°C, precipitates of a new phase with characteristic sizes of ~20 nm form at some stage of the kinetics. Zir-

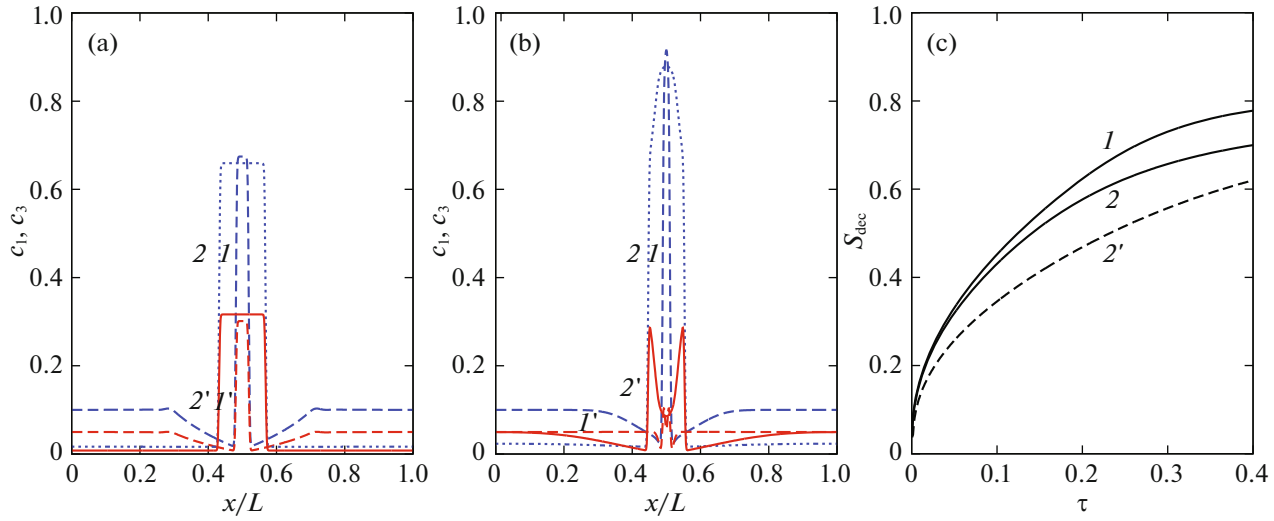

Fig. 2. Kinetics of precipitate growth in an alloy with parameters $\Psi_{12} = \Psi_{23} = 8$, $\Psi_{13} = 0$, $c_{10} = 0.1$, $c_{30} = 0.05$, and $L = 500R$. (a) Distributions of concentrations (*1, 2*) $c_1(x)$ and (*1'*, *2'*) $c_3(x)$ at times τ = (*1*, *1'*) 0.03 and (*2*, *2'*) 0.5 when $D_{ij}^0 = 1$; (b) distributions of concentrations (*1, 2*) $c_1(x)$ and (*1'*, *2'*) $c_3(x)$ at times τ = (*1*, *1'*) 0.01 and (*2*, *2'*) 2.5 when $D_{31}^0 = 10^{-4}$; for all others, $D_{ij}^0 = 1$, $D_{32}^0 = D_{33}^0 = 10^{-2}$, and $D_{ij}^0 = 1$; (c) evolution of decomposition with respect to component **1** for (a) and (b), respectively, and (*1, 2*) when $D_{31}^0 = D_{13}^0 = D_{23}^0 = 10^{-4}$ and $D_{32}^0 = D_{33}^0 = 10^{-2}$; for all others, $D_{ij}^0 = 1$ (*2'*).

conium is missing from the bulk of the precipitates, while its concentration near their surfaces is as high as 15 at %. In contrast, there is no scandium near the surfaces of precipitates, while its concentration in the bulk of precipitates is as high as 25 at %. It should be emphasized that a dispersed state with a high density of fine precipitates was achieved in the three-component alloy, testifying to the mutual influence of Sc and Zr impurities.

The authors of [19] proposed an explanation of this effect using results from kinetic Monte Carlo (KMC) modeling of an alloy's decomposition with energy parameters based on first-principle calculations. The alloy has a thermodynamic tendency to decompose with the formation of precipitates of a partially ordered $Al_3Zr_xSc_{1-x}$ phase in which $0 < x < 1$. The ratio of coefficients of diffusion $D_{Sc}^M \gg D_{Zr}^M$ is established in the initial homogeneous alloy ($\sim 10^3$ at $T = 450$°C), so precipitates supersaturated with scandium form at the first stage. Zr atoms are redistributed at the next stage and migrate to the precipitates. For kinetic reasons, they cannot penetrate deeply into their bulk during an experiment, since the energy of activation for diffusion is high in the bulk of the ordered phase. The coefficient of diffusion of zirconium in the volume of the precipitate is therefore much lower than in the matrix: $D_{Zr}^P \ll D_{Zr}^M$. Based on ab initio calculations of the energy of activation, there is virtually no diffusion in the bulk of the precipitates of the ordered phase, so local thermodynamic equilibrium is not reached during an experiment [19]. The coefficient of diffusion of scandium through the shell is thus much lower than the corresponding one in the matrix: $D_{Sc}^P \ll D_{Sc}^M$. The exchange of Zr atoms between the precipitates is therefore blocked, and a kinetically metastable dispersed state of the alloy is obtained. The authors of [19] also showed that nonequilibrium shells do not form around the precipitates if the coefficients of diffusion of impurities in the matrix and volume of precipitates are assumed to be identical when modeling decomposition according to KMC.

The estimate obtained on the basis of the calculations in our model (Figs. 1 and 2), indicating that a difference of 2–4 orders of magnitude between coefficients of diffusion D_{ij}^0 is needed to observe nonequilibrium shells around precipitates, is thus plausible for some systems. At the same time, our model does not allow us to correctly describe decomposition in Al–Sc–Zr alloy, since it does not consider the energy parameters responsible for ordering.

Let us now consider a disordered Cu–Ag–Ni alloy, in which we believe the considered effects can be expected. We estimate the ratios of thermodynamic and kinetic parameters corresponding to this alloy in our model. It is well known that binary Cu–Ni alloy forms a continuous series of solid solutions at $T >$ 800 K and has wide regions of mutual solubility of the components even at lower temperatures [32]. The Ag and Ni components are virtually immiscible in the solid state even at $T = 1200$ K [33], and the mutual solubility of the Ag and Cu components at $T = 1000$ K is ~5 at % [33]. This means that at $T \sim 800$ K, the following ratio of energy parameters is observed for Cu–Ag–

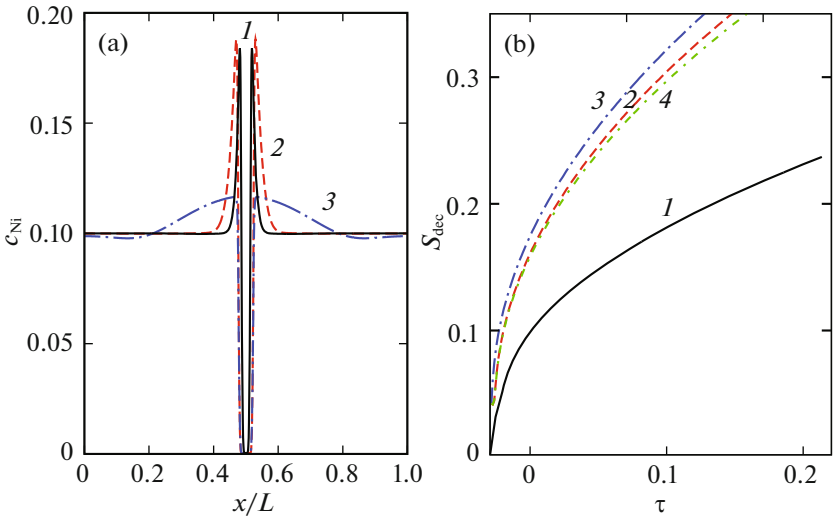

Fig. 3. (a) Distribution of nickel according to time $\tau = 0.15$ in (*1*) $Cu_{80}Ag_{10}Ni_{10}$ alloy with realistic parameters and the same alloy, assuming that (*2*) $D_{Ag(Ni,Cu)\_in\_Ni} = D_{Ag(Ni,Cu)\_in\_Cu}$ and (*3*) $D_{Ni\_in\_Cu} = D_{Ni\_in\_Ag}$; (b) corresponding degrees of decomposition for silver as a function of time. Curve *4* corresponds to decomposition without nickel.

Ni alloy: $\Psi_{AgNi} \gg 1$, $\Psi_{AgCu} \gg 1$, $\Psi_{AgNi} \gg \Psi_{CuNi}$. Ignoring the concentration dependence of these values, CALPHAD data show that we have $\Psi_{AgNi} = 16$, $\Psi_{AgCu} = 8$, $\Psi_{CuNi} = 2.8$ at $T = 800$ K [33].

Let us estimate the values of coefficient of diffusion D_{ij}^0 (m^2/s) based on the experimental data in [34] for $T = 800$ K:

$$D_{Ni\_in\_Ag} = 9.6\times10^{-18}, \quad D_{Cu\_in\_Ag} = 5.6 \times 10^{-17},$$

$$D_{Ag\_in\_Ag} = 4.4\times10^{-17}, \quad D_{Ni\_in\_Cu} = 1.5\times10^{-19},$$

$$D_{Cu\_in\_Cu} = 2.4\times10^{-18}, \quad D_{Ag\_in\_Cu} = 1.2\times10^{-17},$$

$$D_{Ni\_in\_Ni} = 1.1\times10^{-22}, \quad D_{Cu\_in\_Ni} = 1.3\times10^{-21},$$

$$D_{Ag\_in\_Ni} = 3.1\times10^{-22}.$$

We assume that in the initially homogeneous alloy, the concentration of copper is much higher than those of silver and nickel. At the first stage, we would then expect the formation of Ag precipitates due to depletion of this component of the initial matrix. Since Ag and Ni have almost zero mutual solubility, and the coefficients of diffusion of Ni in silver and Ag in copper are approximately the same, we would expect that Ni atoms are quickly displaced from the bulk of the precipitates into the matrix during the formation and growth of precipitates. The mobility of Ni atoms in the copper matrix is then two orders of magnitude lower than in the bulk of the silver precipitates, as can be seen from the reference values of the coefficient of diffusion. We would therefore expect blurred nonequilibrium shells in which the concentration of Ni is much higher than in the bulk of the matrix to form around the precipitates at the initial stages of decomposition, where they grow rapidly. The flow of Ni atoms from the bulk of the precipitates into the matrix is reduced in the late stages of decomposition, where the growth rate of Ag precipitates also slows. The maximum concentration of Ni in the shell starts to fall, and the alloy evolves to an equilibrium state in which Ni is uniformly distributed in the matrix. This situation corresponds qualitatively to the decomposition scenario presented in Fig. 1b. Note too that since the coefficient of diffusion of Ag in nickel is four orders of magnitude lower than that of Ag in copper, we would expect the nickel-enriched shells around Ag precipitates to slow decomposition in the Ag–Cu subsystem in its intermediate stages.

Figure 3 shows results from calculations for $Cu_{80}Ag_{10}Ni_{10}$ alloy using the above parameters. As in Figs. 2a and 2b, the initial state of the alloy was assumed to be uniform with a small perturbation (in this case for silver) in the center of the computational domain. Figure 3a shows the distribution of Ni at time $\tau = 0.15$ (curve *1*); Fig. 3b shows the evolution of decomposition with respect to Ag (curve *1*). We can see the distribution of Ni is largely nonuniform, so its maximum concentration (reached near the precipitation of silver) is approximately twice that of the average for the sample (i.e., a nonequilibrium shell appears around silver precipitates). Based on size $L = 500R$ of the computational region and width ~1 nm of the interface, we can estimate the characteristic time of ~800 s using the formula $\tau = tD_{11}^0/L^2$. Curves *2* and *3*, plotted for an alloy with changed coefficient of diffusions, are also shown for comparison. Curve *2* was plotted by assuming the coefficients of diffusion of the components in nickel do not differ from the corresponding one in the copper matrix, $D_{Ag(Ni,Cu)\_in\_Ni} =$

$D_{Ag(Ni,Cu)\_in\_Cu}$. We can see that nickel-enriched shells still form around the silver precipitates, but degree of decomposition $S_{dec} \sim 0.2$ with respect to silver is reached approximately three times faster. Curve *3* was constructed under the additional assumption that nickel also diffuses in copper at the same rate as in silver: $D_{Ni\_in\_Cu} = D_{Ni\_in\_Ag}$. We can see that no nonequilibrium shell is in this case observed, and the rate of decomposition with respect to silver grows even more. Finally, curve *4* in Fig. 3b was constructed with no nickel in the alloy, and the evolution of decomposition differed little from the last two examples (curves *2* and *3*). We may therefore state that according to our estimates, nickel-enriched nonequilibrium shells around silver precipitates should slow the growth of silver precipitates in $Cu_{80}Ag_{10}Ni_{10}$ alloy by around three times at $T = 800$ K.

CONCLUSIONS

A microscopic approach was used to obtain expressions for the flows of atoms in a three-component disordered alloy that allowed us to study nonequilibrium states during the decomposition of an alloy, including unsaturated precipitates and the formation of shells around the precipitates at intermediate stages of decomposition. It was shown that a nonequilibrium shell can strongly slow the growth of precipitation if the coefficients of diffusion of an alloy's components are lowered in it.

FUNDING

This work was performed as part of State Task "Structure," no. AAAA-A18-118020190116-6.

CONFLICT OF INTERESTS

The author declares he has no conflict of interest.

REFERENCES

1. F. W. Gayle and M. Goodway, Science (Washington, D.C.) **266**, 1015 (1994).
2. F. Suna, J. Y. Zhang, P. Vermaut, et al., Mater. Res. Lett. **5**, 547 (2017).
3. S. Jiang, H. Wang, Y. Wu, et al., Nature (London, U.K.) **544** (7651), 460 (2017).
4. W. C. Leslie and E. Hornbogen, in *Physical Metallurgy,* Ed. by R. W. Cahn and P. Haasen (North-Holland, Amsterdam, 1996).
5. S. Vaynman, R. S. Guico, M. E. Fine, and S. J. Manganello, Metall. Trans. A **28**, 1274 (1997).
6. M. Perez, F. Perrard, V. Massardier, et al., Philos. Mag. **85**, 2197 (2005).
7. P. L. Mangonon, Metall. Trans. A **7**, 1389 (1976).
8. Z. B. Jiao, J. H. Luan, M. K. Miller, et al., Mater. Today **20**, 142 (2017).
9. M. D. Mulholland and D. N. Seidman, Acta Mater. **59**, 1881 (2011).
10. P. Michaud, D. Delagnes, P. Lamesle, et al., Acta Mater. **55**, 4877 (2007).
11. D. J. Ha, H. K. Sung, J. W. Park, and S. Lee, Metall. Mater. Trans. A **40**, 2568 (2009).
12. L. Schemmann, S. Zaefferer, D. Raabe, et al., Acta Mater. **95**, 386 (2015).
13. J. Christian, *The Theory of Transformations in Metals and Alloys*, Part 1: *Equilibrium and General Kinetic Theory* (Pergamon, Oxford, 1975).
14. R. Becker, Proc. Phys. Soc. **52**, 71 (1940).
15. J. W. Cahn and J. E. Hilliard, J. Chem. Phys. **28**, 258 (1958).
16. J. W. Cahn, Acta Metall. **9**, 795 (1961).
17. I. M. Lifshits and V. V. Slyozov, J. Phys. Chem. Solids **19**, 35 (1961).
18. L. Q. Chen, Acta Metall. Mater. **42**, 3503 (1994).
19. E. Clouet, L. Lae, T. Epicier, et al., Nat. Mater. **5**, 482 (2006).
20. S. Ghosh, A. Mukherjeez, T. A. Abinandanan, and S. Bose, Phys. Chem. Chem. Phys. **19**, 15424 (2017).
21. M. S. Bhaskar and T. A. Abinandanan, Comp. Mater. Sci. **146**, 73 (2018).
22. I. K. Razumov and Yu. N. Gornostyrev, Phys. Solid State **61**, 2493 (2019).
23. Ya. E. Geguzin, *Diffusion Zone* (Nauka, Moscow, 1979) [in Russian].
24. I. K. Razumov, Fiz. Tverd. Tela **64**, 19 (2022).
25. A. D. Smigelskas and E. O. Kirkendall, Trans. Am. Inst. Min. (Metall.) Eng. **171**, 130 (1947).
26. V. L. Gapontsev, I. K. Razumov, Yu. N. Gornostyrev, A. E. Ermakov, and V. V. Kondrat'ev, Phys. Met. Metallogr. **99**, 365 (2005).
27. I. K. Razumov and Yu. N. Gornostyrev, in *Proceedings of the 4th School-Seminar on Phase and Structural Transformations in Steels* (Magnitogorsk, 2006), p. 99.
28. I. K. Razumov, Yu. N. Gornostyrev, and A. Ye. Yermakov, J. Alloys Compd. **434–435,** 535 (2007).
29. *Interdiffusion Processes in Alloys,* Ed. by K. P. Gurov (Nauka, Moscow, 1973) [in Russian].
30. S. V. Terekhov, Tech. Phys. **52**, 998 (2007).
31. I. K. Razumov, J. Eng. Phys. Thermophys. **81**, 826 (2008).
32. Y. Iguchi, G. Katona, C. Cserhati, et al., Acta Mater. **148**, 49 (2018).
33. X. J. Liu, F. Gao, C. P. Wang, and K. Ishida, J. Electron. Mater. **37**, 210 (2008).
34. *Landolt-Börnstein: Numerical Data and Functional Relationships in Science and Technology, New Series, Group III: Crystal and Solid State Physics,* Vol. 26: *Diffusion in Metals and Alloys,* Ed. by H. Mehrer (Springer, Berlin, 1990).

Translated by Sh. Galyaltdinov